4th International Conference on Molten Slags and Fluxes, 1992, Sendai, ISIJ

PHYSICAL MODEL OF SLAG FOAMING

Yuji Ogawa*, Didier Huin**, Henri Gaye** and Naoki Tokumitsu*

*Steelmaking Process, Process Technology Research Laboratories, Technical Development Bureau, Nippon Steel Corporation, Japan

**Physical Chemistry Department, IRSID, France

Synopsis: Physical model of slag foaming was developed by using results of cold and hot model experiments. The bubble size at the slag/metal interface, the void fraction of foam and the film life of a bubble at the top surface of slag were calculated. The governing factors of slag foaming have been clarified with this model. It was confirmed that the bubble size at the slag/metal interface is determined basically by the static balance between the buoyancy force ant the adhesive force to the slag/metal interface. It was resulted that the slag/metal interfacial tension and the surface tension of metal also affect the foam height besides the surface tension and the viscosity of slag because they change the bubble size.

Keywords: slag foaming, foam, slag, metal, interfacial tension, contact angle, viscosity

1. Introduction

Slag foaming has been intensively investigated in various steelmaking processes such as converter process, bath smelting, hot metal treatment and electric arc furnace.

But quite a few models of slag foaming have been proposed. Tatsukawa et al. [1] proposed an empirical equation which describes the change in foam height in BOF process. This model is simple and effective to use. However, the knowledge of the average foam life is necessary to predict the foam height. Ito and Fruehan [2],[3] introduced a foaming index which can be obtained from the slag properties. The slag height in the bath smelting and the electric arc furnace processes can be predicted with this model [3]. The coefficient of this model must be measured with each slag because it is an empirical model.

In this study, the authors have tried to make up a slag foaming model with clear physical background. Phenomena in three stages of slag foaming were described based on the previous X-ray fluoroscopic observations [4] and two kinds of water model experiments. With these physical models, the governing factors of slag foaming were investigated.

2. Model

2.1. Concept of slag foaming model

The slag foaming phenomenon is divided into the following three principal stages, by X-ray fluoroscopic observations [4].

1)Formation of CO bubbles at the slag/metal interface and their detachment,
2)Rise of the bubbles in the slag layer and their accumulation under the free surface (formation of the foam),
3)Coalescence of bubbles in the foam and the rupture of bubble films at the top surface of the slag.

The physical model should correspond to these stages.

Fig.1 schematically shows the concept of the present model. The foam height is determined by the

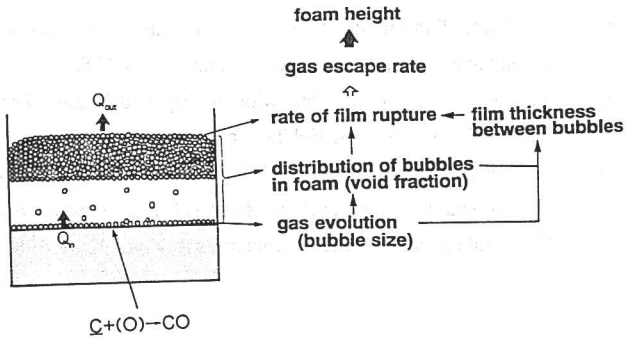

Fig.1. Concept of present foaming model of slag.

balance of the gas evolution rate at the slag/metal interface and the gas escape rate at the top surface of the slag. In this study, the works were concentrated to make clear the governing factors of the gas escape rate.

The gas escape rate is determined by the rupture rate of bubble films at the top surface of slag, the size and the number of the bubbles. The rate of bubble rupture may be governed by the bubble size, the film thickness between bubbles and physical properties of the slag. Moreover, the number of bubbles and the film thickness in the foam are considered to be determined by the gas evolution rate, the bubble size and the slag properties. Therefore, if the bubble size, the distribution of bubbles in the foam and the rupture rate of bubble films at the top surface of the slag are known, the foam height can be predicted.

Mathematical modeling in each stage of slag foaming was constructed as follows:

1) a model to calculate the size of bubbles evolved at the slag/metal interface,
2) a model to estimate the distribution of bubbles in the foam,
3) a model to calculate the rate of film rupture at the top surface of the slag.

2.2. Size of CO bubbles at the slag/metal interface

The size of CO bubbles at the slag/metal interface was assumed to be determined by the static balance of the three interfacial tensions and the static pressure.

The calculations of the configuration of a bubble at the slag/metal interface are based on the resolution of Laplace's equation of capillarity. This equation expresses the difference of pressure across the interface between two phases 1 and 2.

$$\Delta P = \gamma_{12} (1/R_1 + 1/R_2) \tag{1}$$

where γ_{12} is the interfacial tension between the two phases and R_1 and R_2 are the two principal radii of curvature of the interface.

At equilibrium this pressure difference is balanced by the difference of static pressure, which is a function of the position on the interface, the difference between the densities of the two phases and the gravity. If the descending vertical axis is called Oz, this balance gives at any point of the interface:

$$\Delta P = \gamma_{12} (1/R_1 + 1/R_2) = (\rho_1 - \rho_2) g (z - z_O) + \gamma_{12} (1/R_{1O} + 1/R_{2O}) \tag{2}$$

where, ρ_1 and ρ_2 are the densities of the two phases, g is the gravity acceleration and O is a point of reference where the principal radii of curvature are known.

At the joining point of the three phases, the three force vectors of interfacial tensions may be balanced as shown in **Fig.2**.

The contours of gas/slag, gas/metal and slag/metal interfaces were calculated on the basis of the above theory. The configuration in which the slag/metal interface far from the bubble becomes flat was numerically determined by successive approximations. The maximum volume of a bubble which exists stably at the flat slag/metal interface can also be obtained. It was assumed that this volume is that of a bubble just before detachment from the slag/metal interface. The size of a bubble evolved at the slag/metal interface was obtained from this maximum volume, assuming that the bubble after detachment is spherical.

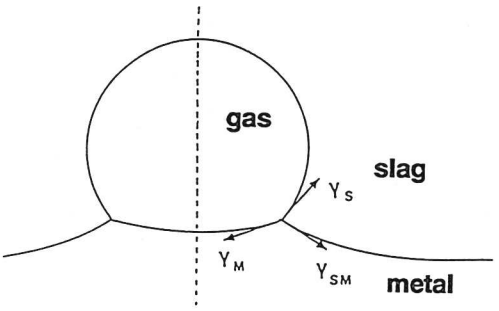

Fig.2. Schematic drawing of a bubble at the slag/metal interface.

2.3. Bubble distribution in the slag layer

The X-ray observations of slag foaming showed the emergence of two superposed layers in the slag: the foam layer and the dispersed gas layer [4]. This behavior is typical two-phase flows. Thus it seems possible to analyze the foaming phenomenon with the help of two-phase flow correlations.

Wallis [5] proposed a theoretical model to describe two-phase flows in a vertical pipe. He assumed that the velocity profile in the pipe is flat and the rise velocity W_∞ of a bubble in an infinite liquid medium follows the modified Stokes law:

$$W_\infty = (\rho_L - \rho_G) g R^2 / 3 \mu_L \tag{3}$$

where ρ_L and ρ_G are the densities of liquid and gas, μ_L is the viscosity of liquid and R is the radius of the bubbles.

From the relationship between the actual and the superficial velocities of gas phase, two values of void fraction (α_1 and α_2) which correspond to two layers are theoretically obtained.

$$\alpha_1 = (1 + \sqrt{1 - 4 J / W_\infty}) / 2 \quad \text{and} \quad \alpha_2 = 1 - \alpha_1 \tag{4}$$

where J is the superficial velocity of gas phase (ratio of gas flow rate to cross section area). The diagram proposed by Wallis (**Fig.3**) gives directly the two values of void fraction.

Thus, this model allows to estimate the void fraction in the two parts of the flow. In the present study, the ability of Wallis model to describe the void fraction in foam was verified.

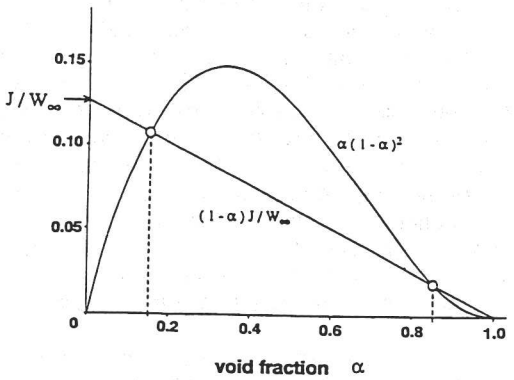

Fig.3. Wallis diagram[5].

2.4. Rupture of bubble films at the top surface of slag

As mentioned before, if the film life of single bubble at the top surface of the foam is estimated, the gas escape rate from the foam can be evaluated as function of the number and the size of the bubbles. However, it is difficult to calculate directly the rate of film rupture of a bubble at the top of the foam. Therefore, in the present model, it was assumed that the film life of a bubble at the top of the foam is the same as that at the top surface of slag without foam.

VOF (Volume Of Fluid) method [6] was adopted to the calculation of film rupture of the bubble. In this method, the free surface is treated by introducing a function F which is the fractional volume of the cell occupied by fluid. By calculating F, the new free surface orientation in each cell is determined. In the cell with F value between zero and unity, the curvature of the free surfaces are obtained from F values of neighboring cells. The pressure and velocity field are calculated with use of the surface tension of liquid and this curvature.

The flow of slag around a bubble at the top surface of the slag was calculated with the VOF method. The bubble was fixed to be spherical and the size was ranged from 2 to 6 cm in diameter, because of difficulty in convergence for smaller bubbles. The initial position of slag surface was taken as 1.5 cm above the top of the bubble. The average decreasing rate in film thickness from 5 to 0 mm at the apex of the bubble was calculated. Although the effect of the bubble deformation is ignored and the bubble size is large, this calculation will be available to evaluate the effects of slag properties and the bubble size on the rate of film rupture,

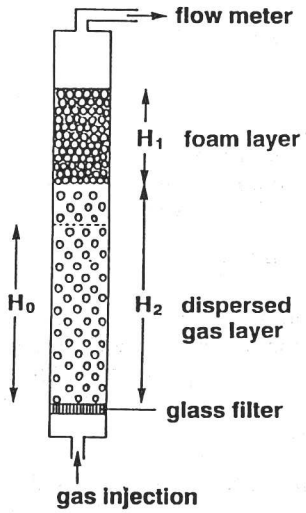

Fig.4. Schematic representation of the water model.

3. Water model experiment

Two kinds of water model experiments with gas bubbling as shown in **Fig.4** were performed. Experiment I is to verify the ability of the Wallis model to describe the foaming phenomenon. Experiment II is to know the difference of film life of a bubble at the top of foam from that at the top surface of the slag without foam.

In experiment I, an initial height H_0 of liquid (water + saccharose) was put in a vertical cylindrical tube (about 1 m in height, inner diameter of 37 mm). Nitrogen gas was injected at the bottom through a glass filter. In order to reduce the bubble coalescence at the outset of the glass filter, 2% ethanol was added in water [7]; the size of the bubbles was much larger (about 5 mm in diameter) without ethanol. The void fractions in the two layers were evaluated by the height of the layers H_1 and H_2.

In experiment II, argon gas was injected into aqueous solution containing 1% gelatin. The diameter of the cylinder was 60 mm and the four kinds of glass filters which have different size of pores were used. The foaming phenomenon was recorded by using a high speed camera (400 frames/sec). The foam height and the bubble size was measured with these images. After the gelatin solution was foamed, gas supply was stopped and the change in the height of solution was measured.

4. Principal results and Discussion

4.1. Bubble size at the slag/metal interface

From the calculation of the bubble at the slag/metal interface, it was found that the critical size of bubbles was dependent on all of three interfacial tensions.

Fig. 5 shows the effect of the contact angle on the bubble size by changing the slag–metal interfacial tension. The critical diameter of bubbles increased almost linearly with the increase in the contact angle. The

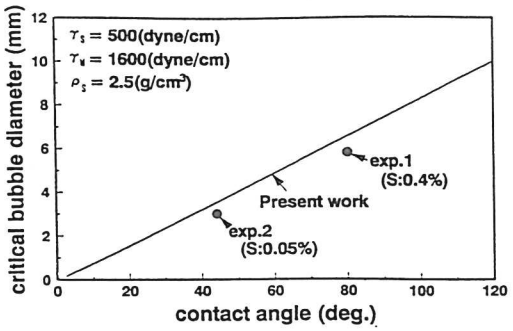

Fig.5. The effect of the contact angle between slag and metal on the critical bubble size.

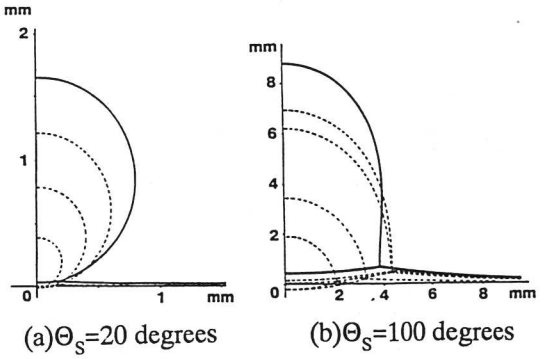

Fig.6. Successive calculated contours of a bubble growing at the slag/metal interface.

relationship between the critical bubble diameter measured in the X-ray fluoroscopic observations and the contact angle is also shown in the same figure in the case of two sulphur concentration. The contact angle data used were those obtained by Cramb et al. [8] based on the measurements of Gaye et al [9]. The measured bubble size agreed well with the calculated one with this model.

Cramb et al. showed that the increase in oxygen content and the decrease in sulphur content lower the contact angle between slag and metal. Mukai et al. [10] indicated that the contact angle decreases sharply with increasing the iron oxide content in slag. Therefore, it is concluded that the decrease in the contact angle by these surface-active elements causes the decrease in the bubble size.

Bubble contours during their growth are illustrated in **Figure 6** for two extreme values of contact angle. In the case of low contact angle, the bubble was almost spherical and the gas/metal contact area was small. On the other hand, when the contact angle is large, the bubble is compressed near the bottom and the gas/metal contact area is relatively large. The shape of bubble agreed with that observed in the experiment with X-ray fluoroscopy [4]. Because the buoyancy force may be balanced with the sum of the vertical component of slag/metal interfacial tensions around the joining boundary of the three interfaces, the decrease in the gas/metal contact area will cause the decrease in the force which should be balanced with the buoyancy forces.

The effects of surface tension of slag and metal on the bubble size were also investigated. The bubble size decreased with decreasing the surface tension of slag and with increasing the surface tension of metal.

4.2. Void fraction in foam

In the water model experiment, it was verified at first that the value of W_∞ compatible with the values of α_1 and α_2 remained reasonably constant, which shows that the bubble size is independent of the gas flow rate. Therefore, the bubble size was estimated by assuming that Wallis model is true.

Measurements were made with two kinds of liquid which have different viscosities. The results are presented in the Wallis diagram (**Fig.7**). For comparison with Wallis theory, the curves corresponding to fixed values of bubble radius (0.16 and 0.18 mm) have been drawn in the same figure. The correlation was fairly good. Some coalescence occurred during the rise of bubbles in the column and their size depended on the gas flow rate; this explains the scattered results for high gas flow rate.

From the above results, it was found that the Wallis model can predict the emergence of two flow configurations: dispersed gas layer and foam layer. It was confirmed that Wallis model is applicable to evaluate the void fraction of the foam as functions of the gas evolution rate, the bubble size and the slag properties.

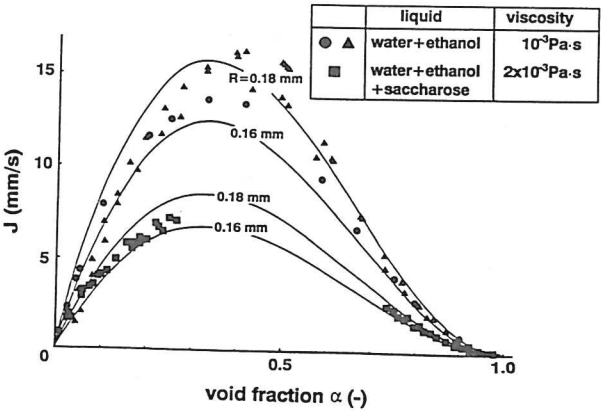

Fig.7. The relationship between the void fraction and the superficial velocity of gas, for two values of viscosity.

4.3. Film life of a bubble at the top surface of slag

4.3.1. Water model experiment

In the experiment with gelatin solution, the average bubble size increased with the increase in the pore size. **Figure 8** shows the effect of the average bubble size on the gas escape rate. The gas escape rate was calculated by the foam decline rate after gas supply was stopped. The gas escape rate increased with the increase in the bubble size. In other words, the foam life increases with decreasing the bubble size. The result agreed with the result in the case of molten slag [4].

Gas escape rate was estimated also from the film life of a single bubble (1 mm in diameter) at the top

surface of the liquid without foam. The time from beginning of the surface deformation by the effect of the bubble rise to the moment of the rupture of the bubble film was measured. And the number of bubbles at the top surface of foam was estimated by the void fraction obtained in the foaming experiment. The X mark in Fig.8. represents the gas escape rate calculated from the film life and the number of bubbles. The estimated value agreed with that obtained by the foam decline rate. From this result, it is considered that the gas escape rate from the foam can be predicted from the film life of a single bubble at the top surface of liquid without foam.

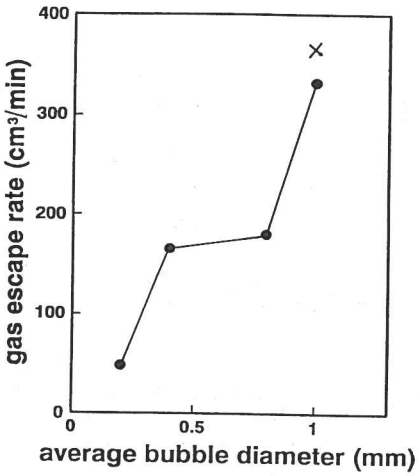

Fig.8. The effect of the average bubble size on the gas escape rate from the foam.

4.3.2. Numerical calculation

Figure 9 shows the configuration when the film thickness becomes zero. The curvature of the slag surface at the apex of the bubble increases with the decrease in the bubble diameter. It is considered that the decrease rate in film thickness is accelerated by the pressure difference between at the apex and near the bottom of the slag surface due to this curvature.

Figure 10 presents the effect of the bubble diameter on the decreasing rate of film thickness. The decreasing rate increased with the decrease in the bubble size below 5 cm in diameter. This may be because of the increase in the pressure difference due to the increase in curvature of the slag surface. In other words, the film life of a single bubble at the top surface of slag increased with the bubble size. But the increasing rate is not so much, while the volume of a bubble is proportional to the third power of the diameter. Thus, total gas escape rate will increase with the increase in the bubble size as observed in the water and X-ray experiments.

The effects of surface tension and viscosity of slag on the rate of the decrease in film thickness were also investigated. The increase in the surface tension of slag enlarged the decreasing rate of film thickness. This may be due to the increase in the pressure difference mentioned above. On the other hand, the slag viscosity reduced the decreasing rate of the film thickness, because the flow in the film may be suppressed.

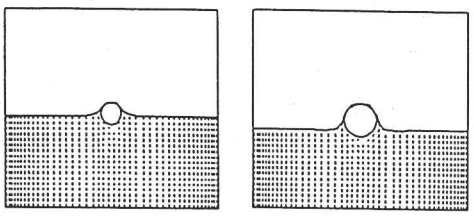

Fig.9. Calculated configuration of the top surface of slag around a bubble just before the film rupture.

4.4. The effects of properties of slag and metal on the foam height

The governing factors of the bubble size evolved at the slag/metal interface, the void fraction in the foam and the rate of film rupture of the bubbles at the top surface of the foam was made clear with the three models of each foaming process. Therefore, the qualitative evaluation of the effects of the physical properties of slag and metal on the foam height could be made.

Table 1 shows the effects of the properties of slag and metal on the foam height. The effect of each property is considered as follows:

<u>viscosity of slag</u>

According to Wallis diagram, the void fraction of foam decreases with increasing the slag viscosity, then the film between two bubbles in the foam may become thick. The downward flow in the film of the bubble at the top surface of the foam may be suppressed by the increase in the slag viscosity. These two effects will cause the increase in the film life of bubbles at the top of the foam and then the increase in the foam height.

<u>surface tension of slag</u>

The bubble size increases with increasing the

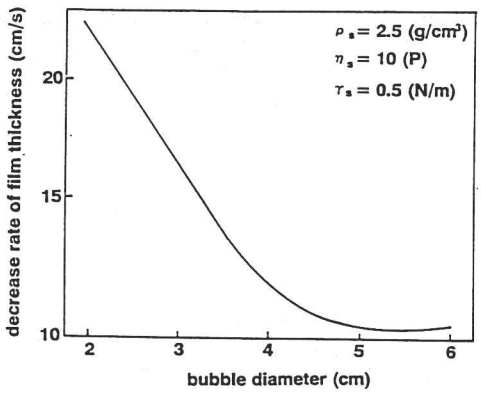

Fig.10. The effect of the bubble diameter on the decreasing rate of the thickness of bubble film.

surface tension of slag. The film between bubbles becomes thin, because the void fraction in foam increases with the increase in the bubble size. The downward flow in the film of the bubble at the top of the foam will be promoted because of the increase in the pressure difference due to the curvature of the slag surface around the bubble. Therefore, the rate of film rupture of the top bubbles will increases with the surface tension of slag and the foam height will decrease.

Table 1. The effects of the properties of slag and metal on the bubble size at the slag/metal interface, the void fraction of foam, the rupture rate of bubble film and the foam height.

	Foam height	Rupture rate of bubble film	Bubble size	Void fraction of foam
Slag viscosity ↑	increase	↓	—	↓
Surface tension of slag ↑	decrease	↑	↑	↑
Slag-metal interfacial tension ↑	decrease	↑	↑	↑
Surface tension of metal ↑	increase	↓	↑	↓

slag/metal interfacial tension

The bubble size increases with the slag/metal interfacial tension. It will also cause the increase in the rate of film rupture of the top bubbles and then the decrease in the foam height.

surface tension of metal

The increase in the surface tension of metal decreases the bubble size. Therefore, the foam height increases with the surface tension of metal.

The effects of viscosity and surface tension of slag on the foam height obtained in this study agree with those of most of the previous works. It has been clarified that the slag/metal interfacial tension and the surface tension of metal also affect the foam height because they may change the bubble size.

5. Conclusion

Physical model of slag foaming was derived by using results of cold and hot model experiments. The governing factors of slag foaming have been clarified more in detail with this model. The effects of the physical properties of slag and metal on the foam height have been made clear. It was confirmed that the bubble size evolved at the slag/metal interface is determined basically by the static balance between the buoyancy force and the adhesive force to the slag/metal interface, and the slag/metal interfacial tension and the surface tension of metal also affect the foam height besides the surface tension and the viscosity of slag through the change in the bubble size.

References

1)M.Tatsukawa, M.Shimada, M.Ishibashi and T.Shiraishi: Tetsu-to-Hagane, 60(1974), A19.
2)K.Ito and R.J.Fruehan: Metall. Trans. B, 20B(1989), 509.
3)K.Ito and R.J.Fruehan: Metall. Trans. B, 20B(1989), 515
4)Y.Ogawa and N.Tokumitsu: Proc. of 6th Int. Iron and Steel Cong. Vol.1, ISIJ, Tokyo, (1990), 147.
5)G.B.Wallis: International Developments in Heat Transfer, ASME, (1963), 319.
6)M.D.Torrey, L.D.Cloutman, R.C.Mjolsness and C.W.Hirt: NASA-VOF2D: A Computer Program for Incompressible Flows with Free Surface, LA-10612-MS, Los Alamos Scientific Laboratory, Los Alamos, New Mexico, (1985).
7)B.J.Ackers: Foams, Academic Press, London, (1976), 147.
8)A.W.Cramb and J.Jimbo: Steel Research, 60(1989), 157.
9)H.Gaye, L.D.Lucas, M.Olette and P.V.Riboud: Can. Metall. Quart., 23(1984), 179.
10)K.Mukai, H.Furukawa and T.Tsuchikawa: Tetsu-to-Hagane, 63(1977), 1484.